Journal of Renewable and Sustainable Energy ARTICLE pubs.aip.org/aip/rse

Design, modeling and simulation of nuclear-powered integrated energy systems with cascaded heating applications

Cite as: J. Renewable Sustainable Energy **15**, 054103 (2023); doi: 10.1063/5.0163557
Submitted: 17 June 2023 · Accepted: 13 September 2023 ·
Published Online: 16 October 2023

Bikash Poudel,[1] Mukesh Gautam,[1] Binghui Li,[1,a)] Jianqiao Huang,[1] and Jie Zhang[2]

AFFILIATIONS

[1]Idaho National Laboratory, Idaho Falls, Idaho 83415, USA
[2]Department of Mechanical Engineering, The University of Texas at Dallas, Richardson, Texas 75080, USA

Note: This paper is part of the special issue on Hybrid Renewable Energy Systems
[a)]**Author to whom correspondence should be addressed:** binghui.li@inl.gov

ABSTRACT

Nuclear-renewable integrated energy systems (IES) consist of a variety of energy generation and conversion technologies and can be used to meet heterogeneous end uses (e.g., electricity, heat, and cooling demands). In addition to supply-demand balance, end-use heat demands usually require heat supply of certain temperature ranges. The effective and efficient utilization of heat produced within an IES is, therefore, a critical challenge. This paper examines design options of an IES that includes heating processes of multiple temperature grades. We investigate a cascaded design configuration, where the remaining residual heat after high-grade heating processes [e.g., hydrogen production through high-temperature steam electrolysis (HTSE)] is recovered to meet the low-grade heating needs [e.g., district heating (DH)]. Additionally, a thermal energy storage system is integrated into the DH system to address the imbalance between heat supply and demand. This paper primarily focuses on the design and modeling of the proposed system and evaluates its operation with a 24-h transient process simulation using a DH demand profile with hourly resolution. The results indicate that the residual heat from the HTSE exhaust is insufficient for the DH demand, and additional topping heat directly from the reactor process steam is needed. Furthermore, the inclusion of thermal energy storage within the DH system provides the necessary balance between thermal generation and demand, thereby ensuring a consistent rated temperature of the DH supply water. This approach helps minimize the control actions needed on the reactor side.

NOMENCLATURE

Acronyms

BOP	balance of plant
DH	district heating
HTSE	high temperature steam electrolysis
HX	heat exchanger
IES	integrated energy system
LWR	light water reactor
MWe	megawatt electric (unit of measurement of electricity produced by the balance of plant or electrical load)
MWth	megawatt thermal (unit of measurement of heat produced by the reactor or heating load)
SG	steam generator
SMR	small modular reactor
SOEC	solid oxide electrolyzer cell
TES	thermal energy storage

Indices

t	index of time

Variables

$c^{p/str}$	specific heat capacity of the DH working fluid/TES storage medium, kJ/(kg · K)
$h_t^{HTSE/DH,ext}$	enthalpy of secondary coolant that exits the heat exchanger of HTSE/DH, J/kg
$h_t^{out/in}$	enthalpy of working fluid that exits/enters the steam turbine, J/kg

m^{str}	mass of the TES storage medium, kg
$\dot{m}^{pipe}$	mass flow rate of the DH supply water, kg/s
$\dot{m}_t^{bv}$	mass flow rate of steam bypassed to the condenser through turbine bypass valve, kg/s
$\dot{m}_t^{BOP/HTSE/DH}$	mass flow rate of steam supplied by steam manifold to BOP/HTSE/DH, kg/s
$\dot{m}_t^{char/dis}$	mass flow rate of the charging/discharging fluid of the TES, kg/s
$\dot{m}_t^{cond}$	mass flow rate of working fluid collected by condenser, kg/s
$\dot{m}_t^{cs}$	steam produced by the steam generators and delivered to the steam manifold, kg/s
$\dot{m}_t^{HX1/HX2}$	mass flow rate of secondary coolant that enters HX1/HX2, kg/s
$\dot{m}_t^{H_2}$	hydrogen production rate, kg/s
$\dot{m}_t^{tur}$	mass flow rate of steam to the steam turbine, kg/s
$\dot{m}_t^{waste}$	mass flow rate of the HTSE exhaust fluid bypaased to the condenser, kg/s
P_t^{HTSE}	electricity consumed by the HTSE process, We
P_t^{mech}	mechanical power, kW
$P_t^{R,th}$	thermal power produced by the reactor, Wth
q_t^{dem}	heat demand, Wth
q_t^{HTSE}	heat absorbed by the HTSE process from the process steam, Wth
$q_t^{HX1/HX2}$	heat absorbed by the DH system through heat exchangers HX1/HX2, Wth
q_t^{TES}	heat transferred to the TES, Wth
$T_{rat}^{DH,in}$	Rated return temperature of the DH system, °C
$T_{rat}^{DH,out}$	rated supply temperature of the DH system, °C
$T_t^{C,out}$	temperature of charging flow that exits TES, °C
$T_t^{DH'}$	temperature of the DH working fluid before entering HX1, °C.
$T_t^{D,in/out}$	temperature of discharging flow that enters/exits TES, °C
$T_t^{DH,in/out}$	temperature of working fluid that exits/enters the DH, °C
T_t^{TES}	temperature of the TES storage medium, °C
Δh_t^{tur}	enthalpy difference across the turbine, J/kg
Δt	simulation time step, s
$\eta^{dis/char}$	TES discharging/charging efficiency
η^{tur}	turbine efficiency

I. INTRODUCTION

The Biden administration has set ambitious decarbonization goals for the whole U.S. economy in 2050.[1] Although total carbon emissions of the electricity sector has dropped significantly, other energy sectors, such as the industry and residential sectors, remain large carbon emitters. In 2022, the residential and industrial sectors accounted for 19% and 21% of the nation's energy-related carbon dioxide (CO_2) emissions, respectively.[2] Particularly, the industrial sector is considered as a "difficult-to-decarbonize" sector, due in part to the diversity and heterogeneity of industrial processes and operations.[3] The generation and conversion of heat accounts for the largest share of energy-related carbon emissions in both sectors: Space heating accounted for 36% of total residential carbon emissions in 2022,[2] and process heating accounted for over 30% of total carbon emissions in the manufacturing industry.[4] Finding carbon-free alternative heat sources is therefore crucial in both sectors, as outlined in the U.S. Department of Energy's industrial decarbonization roadmap.[4]

Nuclear energy is a clean, carbon-free energy source that can provide both electricity and heat. Traditionally nuclear power plants are primarily powered by large light water reactors (LWRs) that are used as base load plants in power systems. In the recent decades, however, nuclear power plants are losing popularity because of safety concerns and because their advantages over other power plants are not valued in electricity markets.[5] Operators of nuclear power plants are, therefore, exploring new paradigms to maximize their economic revenues. Because there is no relevant cost saving in decreasing the electricity production from nuclear power plants, an economic way to utilize excess steam during off-peak periods is redirecting steam for alternative purposes.[6] These applications encompass various areas, including desalination,[7] hydrogen production,[8,9] district heating (DH), and cooling.[6,10–15]

Nuclear-renewable integrated energy systems (IES) include multiple energy resources and conversion technologies to meet end-use demands in a variety of forms, including but not limited to heat and electricity. These systems typically consist of nuclear reactors, renewable energy sources, energy storage systems, and industrial processes that are dynamically dispatched to meet end-use demands while maximizing energy utilization and minimizing environmental impacts.[5,16] Coupled with other carbon-free subsystems, nuclear power can be used to increase system reliability and resilience. For example, although coal and gas dominate the fuels used for district heating historically,[17] several countries already have experience in nuclear district heating.[18] Alternatively, hydrogen has the potential to decarbonize traditionally hard-to-decarbonize sectors.[19,20] It can be used as a reducing agent in place of coal or natural gas in the production of iron and steel or used as a fuel in industrial boilers and furnaces to reduce the reliance on fossil fuels. Although conventionally hydrogen is produced predominantly via steam reforming, which is a carbon-emitting process due to reliance on fossil fuels, electrolysis can be a carbon-free alternative to produce hydrogen at high efficiency and high purity if paired with clean electricity sources.[21]

Unlike electricity, a key consideration in utilization of heat is temperature, as different end-users require different temperature ranges. Most LWRs operate in the region of 300 °C, while the temperature of end-use heat demand varies significantly. For example, district heating requires the temperature of heat supply, typically in the form of steam or hot water, ranging from 60 to 150 °C.[18,22,23] Thermal desalination requires a temperature range between 90 °C (multi-effect distillation[24]) to 110 °C (multistage flash[25]) The temperature requirements of hydrogen production, depending on the specific technology, range from 70 to 80 °C (polymer exchange membrane electrolysis) to over 800 °C (solid oxide electrolysis).[26,27] Technical feasibility must be evaluated before deployment of nuclear-renewable integrated energy systems. For example, Kim *et al.*[8] conducted dynamic analysis of planar solid oxide electrolysis coupled with an LWR and simulated transient response of the integrated system.

Thermodynamics and techno-economic assessments of cascade heat utilization can be found in the existing literature, which is mostly focused on waste heat from fossil-fueled thermal generators.[28]

These studies usually utilize waste heat to power a variety of technologies, including organic Rankine cycles, absorption refrigeration systems, and heat pumps.[29–31] Previous studies have also examined technical feasibility of SMR coupled with hydrogen production[8] and district heating[12,13] separately.

In this study, we model and simulate cascade utilization of steam extracted from small modular reactors (SMRs) for hydrogen production and district heating. SMRs, unlike conventional large reactors with rated capacity greater than 700 MWe, are smaller in size, typically less than 300 MWe, and are factory-manufactured transportable units. They can be utilized in various applications such as electricity generation, desalination, and heat generation. SMR technology offers a variety of advantages over large LWR due to its relatively smaller capacity and modularity. We develop physics model of an IES consisting of a primary heating system (i.e., SMR), a balance of plant (i.e., turbine and synchronous generator), a hydrogen production unit (i.e., industrial process), and a district heating system. We simulate the operations of the proposed IES using Dymola, a transient simulation tool based on Modelica programming language, under a set of operating strategies to evaluate their impacts on system performance.

The remainder of this paper is structured as follows: Sec. II outlines the design of the IES, including the modeling equations and control strategies used in the simulations presented in this paper. Section III presents the simulation results obtained under various operation scenarios. Section IV concludes the study and discusses potential future work.

II. DESIGN, MODELING, AND CONTROL

In this section, we describe the IES analyzed in this paper. The design and integration of IES subsystems are discussed along with their modeling equations. The control framework is provided along with the equations to evaluate the control setpoints for various subsystems.

A. The modeled system

The IES examined in this paper consists of six subsystems: a small modular reactor, a steam manifold, the balance of plant (BOP), a high temperature steam electrolysis (HTSE) process, a district heating network, and a connected electrical grid. HTSE is an industrial process that consumes heat and electricity to produce hydrogen at high temperatures (over 800 °C).[8] By contrast, DH is a low-temperature application that consumes heat to produce hot water (at around 90 °C) to meet the district heating needs.[23] The architecture of IES is depicted in Fig. 1. The arrows in Fig. 1 symbolize the transfer of mass and energy between various subsystems. The presence of heat exchanger interfaces on the SMR, HTSE, and DH systems means that only heat is exchanged between the SMR's secondary coolant flow and these particular subsystems.

To model the system components, we utilize the Modelica programming language within the Dymola environment.[32] Existing transient-process models of the SMR, HTSE, steam turbine, and BOP are used from the HYBRID repository developed by the Idaho National

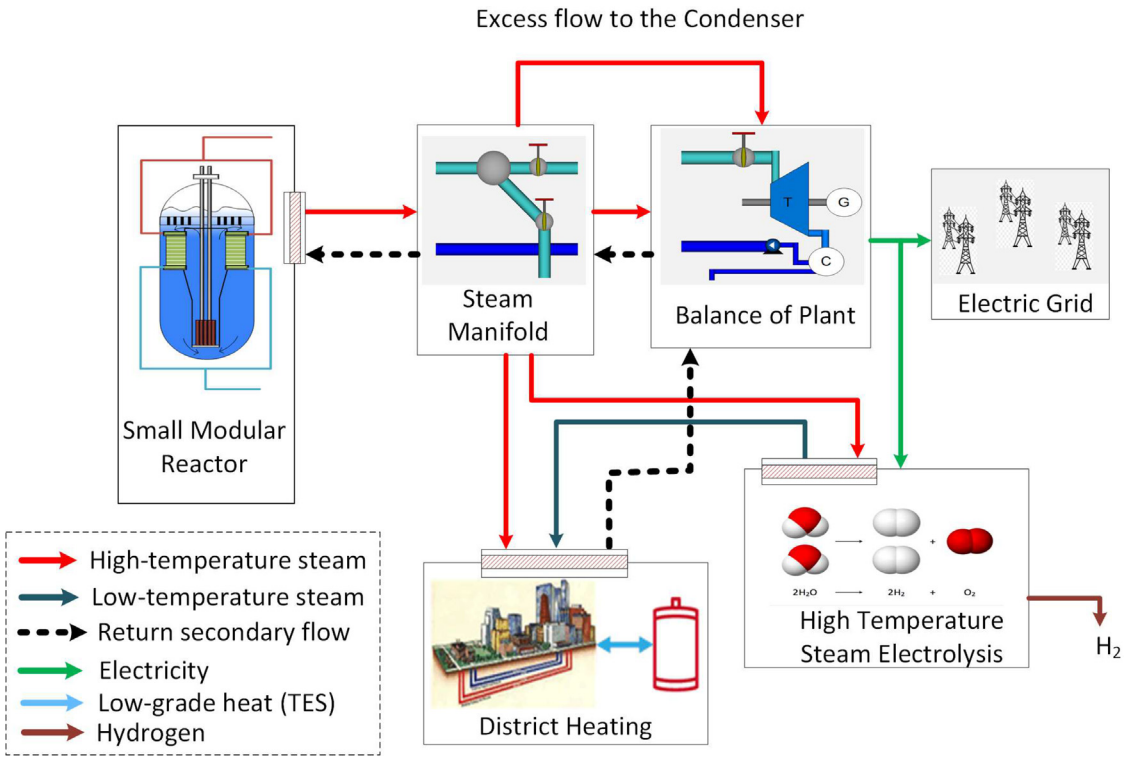

FIG. 1. Block diagram of the IES system. High-temperature process steam is generated in steam generators of the SMR and flows to the steam manifold, which distributes it to the BOP, HTSE, and DH systems. After releasing heat in the end-use devices, the process steam condensed to water, flows back to the SMR steam generator as feedwater, and completes a cycle. Note that the process steam supplies thermal energy to the HTSE and DH systems via heat exchangers and there is no mass exchange.

Laboratory.[33] Furthermore, new models have been developed for the DH system which incorporates a sensible-heat thermal energy storage (TES). These subsystems are detailed in the following subsections:

1. Small modular reactor

SMR serves as the primary energy source for the IES. We employ the NuScale reactor, which is a 60 MWe (200 MWth) LWR-type SMR. This technology is widely recognized as one of the most mature SMR technologies in the United States.[7,34] The heat generated by the SMR through nuclear fission is harnessed to produce high-temperature process steam. The steam is then utilized for electricity generation in the BOP, as well as to provide thermal energy to both the HTSE process and the DH system.

Figure 2 illustrates a cross-sectional view of the NuScale reactor module. The NuScale reactor is a pressurized reactor vessel consisting of the primary coolant system and two steam generators. The primary coolant system includes a reactor core, a pressurizer, a hot-leg riser and a cold-leg downcomer.[35] The reactor core consists of fuel and control rod assemblies. The heat produced inside the core is absorbed by the primary coolant. Two vertical, once-through, helical coil steam generators are situated between the hot leg riser and the outer wall of the reactor module. Secondary coolant feedwater is pumped through these steam generator tubes, extracts heat from the primary side, and produces high-temperature process steam. Through the steam generator metal interface, only heat is transferred from the primary to the secondary coolant, while maintaining mass balance on both sides. The primary coolant circulates passively within the vessel, driven by the natural buoyancy force resulting from temperature variations across the primary coolant circuit.

We utilize an existing Modelica model of NuScale reactor available in HYBRID.[33,35] The modeling details of NuScale reactor can be found in its user manual.[36] Under rated full power conditions (200 MWth), the NuScale reactor produces 84 kg/s of high-temperature steam at 310 °C. The feedwater is supplied at 148 °C and 3.77 MPa.

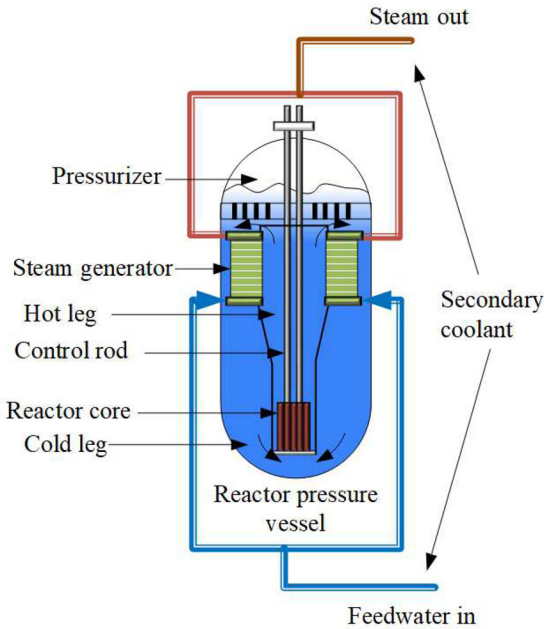

FIG. 2. NuScale SMR module.[13]

2. Steam manifold

The steam manifold comprises splitting volumes, valves, and pipes to distribute the process steam to different downstream IES processes. In our study, the steam manifold distribute steam to three downstream processes: BOP, HTSE, and DH system. The valves are regulated based on the steam demand from the processes.

3. Balance of plant

The BOP encompasses a turbine-generator setup designed to generate electricity using high-temperature steam. The steam turbine extracts thermal energy from the pressurized steam generated inside the SMR and converts it into mechanical work. The synchronous generator then converts this mechanical power into electric power. The generated electricity is either supplied to the HTSE for hydrogen production or directly to the grid. The BOP also includes a turbine control valve to regulate the steam flow to the turbine and a bypass valve that redirects excess steam directly to the condenser. The turbine control valve adjusts based on the electricity demand, while the bypass valve is controlled using a pressure sensor signal.

We leverage an existing BOP model from the HYBRID repository.[33] This model includes additional components such as the condenser, pump, and feedwater heater as part of the BOP subsystem. The condenser receives the exhaust from the steam turbine, the flow from the bypass valve line, and cold returns from the HTSE and DH systems. Its function is to condense the fluid mixture into a liquid phase. The resulting liquid is then pumped, preheated, and supplied to the steam generators of the SMR.

At rated capacity in electricity-only mode, the steam turbine consumes 84 kg/s of high-temperature steam to produce 60 MWe of electricity. The turbine exhaust is maintained at 0.01 MPa (45.8 °C). At such low temperature, the thermal energy remaining in the two-phase mixture at the turbine exhaust is not suitable for any heating applications. The condenser condenses the fluid mixture into liquid state at 0.01 MPa, which is then compressed to 3.77 MPa. The resulting feedwater is preheated to 148 °C and directly supplied to the tube side of the steam generators in the SMR.

4. High temperature steam electrolysis

The HTSE process utilizes heat and electricity to split water into hydrogen and oxygen. This occurs within solid oxide electrolyzer cell (SOEC) stacks comprising cathode, anode, and electrolyte layers.[8,27] The heat available in the high-temperature steam from SMR is employed to preheat de-ionized water to slightly more than 250 °C. Because the required temperatures are 850 °C for both the cathode and anode streams at the SOEC stack inlet, the preheated water is further heated by recovering heat from streams exiting the SOEC stacks (750 °C at both the anode and cathode outlets) and by electrical topping heat, resulting in steam at the desired temperature of 850 °C.[8] The steam is then split into hydrogen and oxygen within the electrolyzer vessel using electrical power.

The HTSE model available in the HYBRID repository[33,37] is utilized, with modifications made to match the steam conditions produced by the SMR. The nominal conditions of the ports, including pressure, temperature, mass flow, etc., are adjusted to align with the steam output from the SMR.

Under nominal conditions, the HTSE system receives 7.23 kg/s of high-temperature process steam from the steam manifold and 53.3 MWe of electricity to produce 0.4 kg/s of hydrogen. Based on our observations from the HYBRID model, the SMR's secondary coolant fluid returning from the HTSE process has a temperature of 230 °C. Therefore, the residual heat in the HTSE return can be recovered and utilized in low-temperature applications such as district heating, which will be discussed in greater detail in Sec. II B.

5. District heating system

The DH system utilizes thermal energy from the IES to meet local heat demands. The DH system distributes hot water through insulated pipelines to deliver heat to end-use residential and commercial facilities. This can include facilities owned by the IES itself, as well as any local consumers that the IES can support.

To enable efficient heat management, the DH system includes a sensible-heat thermal energy storage (TES) system. The TES is an insulated water storage tank designed to store excess thermal energy during periods of low heat demand and dispatch during periods of high demand. The TES is a cylindrical shape stratified thermal storage tank, modeled as four volume segments with a total tank volume of 1000 m^3. The storage medium is vertically arranged in these four layers with different temperatures.[38,39] Water is used as the storage medium to retain and release heat.

The heat demand is modeled as a lumped heat load with a variable flow rate. The supply temperature is maintained at 90 °C, while the return temperature is set at 40 °C. The DH flow rate varies based on the heat demand at different times of day. The DH system can source heat from the topping steam supplied directly by the steam manifold (310 °C) or from exhaust of the HTSE process (230 °C). The design and modeling equations of the DH system are discussed in detail in Sec. II C.

6. Electrical grid

In the HYBRID model, the electrical grid is represented as an infinite source and sink to simulate the behavior of a large grid. Any surplus electricity generated by the IES is absorbed by the electrical grid at market price. Likewise, if the electricity produced by the BOP is insufficient to meet the electricity demand of the HTSE process, additional electricity is drawn from the grid to compensate for the deficiency.

B. Cascaded heating design

The IES analyzed in this paper includes two heat applications: HTSE and DH. HTSE operates at high temperature, while DH operates at low temperature. As discussed in Sec. II A, there is residual heat at the exhaust of HTSE process which can be recovered and utilized for district heating. Note that the HTSE exhaust here refers to the SMR secondary coolant fluid returning back from the HTSE after pre-heating the water undergoing electrolysis inside the HTSE vessel.

Based on our observations from the HYBRID model, the coolant return at the HTSE exhaust has a temperature of 230 °C. According to our simulations, average of 270 kJ of heat can be recovered by the DH system for each kilogram of fluid from the HTSE exhaust.

Based on this information, we design the IES in a cascaded heating configuration, where the HTSE and DH systems are connected in a tandem structure. The HTSE system receives the direct process steam from the steam manifold, while the DH system is fed with the fluid return from the HTSE exhaust. The DH system also receives a direct supply of steam from the steam manifold to provide the topping heat, but this is only used when the heat available from HTSE is insufficient. The DH system is thus equipped with two heat exchangers (HXs): one to recover heat from the HTSE exhaust and another to provide topping heat from a portion of the steam extracted directly from the steam manifold (Fig. 3). Further details on DH system model will be discussed in Sec. II C.

C. Mathematical formulation

This subsection focuses on the modeling of the district heating system and its integration with other components of the IES. Since we are utilizing existing SMR, BOP, HTSE, and electrical grid models from the HYBRID repository, we have excluded their detailed modeling in this paper.

1. Steam manifold and secondary coolant

The preheated feedwater enters the tube side of the steam generator (SG), undergoes a phase change, and transforms into steam by absorbing heat from the primary coolant. This heat is equivalent to the thermal power generated within the reactor core. Therefore, the

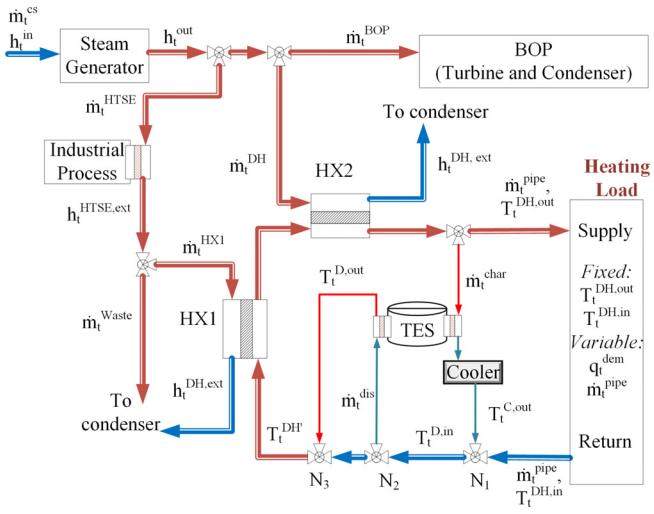

FIG. 3. Mass and energy flow in the DH system. Two heat exchangers, HX1 and HX2, are used to transfer heat to the DH system from HTSE exhaust and topping steam, respectively. A sensible-heat TES is used to store surplus heat during periods of low demand and release it when demand is high.

thermal power produced in the reactor core and delivered to the secondary coolant can be expressed as follows:

$$P_t^{R,th} = \dot{m}_t^{cs}(h_t^{out} - h_t^{in}). \quad (1)$$

The resulting steam generated by the SG is received by the steam manifold and is distributed to the HTSE, DH, and BOP systems. The mass flow balance in steam manifold is given as follows:

$$\dot{m}_t^{cs} = \dot{m}_t^{BOP} + \dot{m}_t^{HTSE} + \dot{m}_t^{DH}. \quad (2)$$

Within the BOP, a turbine valve is operated to regulate steam flow to the steam turbine, and the excess steam is redirected to the condenser using a bypass valve ($\dot{m}_t^{bv}$). The mass flow distribution inside the BOP is

$$\dot{m}_t^{BOP} = \dot{m}_t^{tur} + \dot{m}_t^{bv}. \quad (3)$$

The steam turbine converts thermal energy into mechanical power (P_t^{mech}). The mechanical power is, therefore, a function of enthalpy difference across the turbine (Δh_t^{tur}) and steam flow rate ($\dot{m}_t^{tur}$),

$$P_t^{mech} = \eta^{tur}\Delta h_t^{tur}\dot{m}_t^{tur}. \quad (4)$$

The amount of hydrogen produced by the HTSE process is a function of heat extracted from process steam and consumed electricity,[8,40]

$$q_t^{HTSE} = \dot{m}_t^{HTSE}(h_t^{out} - h_t^{HTSE,ext}), \quad (5)$$

$$\dot{m}_t^{H_2} = f(P_t^{HTSE}, q_t^{HTSE}). \quad (6)$$

The condenser located inside the BOP receives the return flow from turbine, bypass valve, DH system, and HTSE (flown through the DH system). The mass flow received by the condenser ($\dot{m}_t^{cond}$), therefore, equals $\dot{m}_t^{cs}$:

$$\dot{m}_t^{cond} = \dot{m}_t^{cs} = \dot{m}_t^{tur} + \dot{m}_t^{bv} + \dot{m}_t^{DH} + \dot{m}_t^{HTSE}. \quad (7)$$

2. District heating system model

The configuration of DH system is illustrated in Fig. 3. The DH system, including of two HXs in a cascade, is capable of utilizing heat from two different sources. The first heat exchanger, HX1, recovers the heat from the exhaust of the HTSE, while the second heat exchanger, HX2, provides the topping heat to meet the DH supply temperature requirements. A direct bypass line is also provided to HX1 to divert the flow directly to a condenser bypassing DH system ($\dot{m}_t^{waste}$) in case the heat available in HTSE exhaust exceeds the DH system demand. The mass flow balance equation for the HTSE exhaust line can be expressed as

$$\dot{m}_t^{HTSE} = \dot{m}_t^{HX1} + \dot{m}_t^{waste}. \quad (8)$$

The heating fluid supplied to HX2 is the topping steam extracted from steam manifold for the DH system

$$\dot{m}_t^{HX2} = \dot{m}_t^{DH}. \quad (9)$$

The thermal power extracted from the HTSE exhaust and topping steam in HX1 and HX2, respectively, are given by

$$q_t^{HX1} = \dot{m}_t^{HX1}(h_t^{HTSE,ext} - h_t^{DH,ext}), \quad (10a)$$

$$q_t^{HX2} = \dot{m}_t^{HX2}(h_t^{out} - h_t^{DH,ext}). \quad (10b)$$

The DH system includes a dedicated sensible-heat TES in the form of a hot water storage tank. The TES stores excess heat during low-demand periods and releases heat during high-demand periods. Separate structures are incorporated within the TES for charging and discharging.

The amount of heat absorbed and released by the TES during charging and discharging processes dependents on the temperature of the TES at a given time. During the charging process, a fraction of the hot water exiting from HX2, denoted as $\dot{m}_t^{char}$, is directed to the TES. The charging flow supplied to the TES at temperature $T_t^{DH,out}$ returns at $T_t^{C,out}$. This flow then combines with the flow returning from the DH load at flow node N1, elevating the temperature to $T_t^{D,in}$.

During the discharging phase, a portion of feedwater, denoted as $\dot{m}_t^{dis}$, is supplied to the TES for preheating. The discharging flow is supplied to the TES at temperature $T_t^{D,in}$ and returns at $T_t^{D,out}$. This preheated portion of feedwater then combines with the remaining flow at node N3, raising the temperature of the feedwater entering HX1 to $T_t^{DH'}$. The average temperature of the TES can be calculated as

$$q_t^{TES} = c^p(\dot{m}_t^{char}(T_t^{DH,out} - T_t^{C,out}) - \dot{m}_t^{dis}(T_t^{D,out} - T_t^{D,in})), \quad (11a)$$

$$T_{t+1}^{TES} = T_t^{TES} + \int_0^{\Delta t} \frac{q_t^{TES}}{c^{str}m^{str}}dt. \quad (11b)$$

Note that there are four layers of storage medium inside the TES. The temperature described by (11b) is the average across all four layers. The resulting temperatures of DH pipeline water at different heating stages are as follows:

$$T_t^{D,in} = \frac{T_t^{DH,in}\dot{m}_t^{pipe} + \dot{m}_t^{char}T_t^{C,out}}{\dot{m}_t^{pipe} + \dot{m}_t^{char}}, \quad (12a)$$

$$T_t^{DH'} = \frac{\dot{m}_t^{dis}T_t^{D,out} + (\dot{m}_t^{pipe} + \dot{m}_t^{char} - \dot{m}_t^{dis})T_t^{D,in}}{\dot{m}_t^{pipe} + \dot{m}_t^{char}}, \quad (12b)$$

$$T^{DH,out} = T_t^{DH'} + \frac{q_t^{HX1} + q_t^{HX2}}{c^p(\dot{m}_t^{char} + \dot{m}_t^{pipe})}. \quad (12c)$$

For modeling simplicity and control flexibility, a cooler is placed in the charging line between the TES and node N1. This cooler will lower the temperature of charging flow return down from $T_t^{C,out}$ to $T_t^{DH,in}$, which is set at 40 °C for the purpose of this paper. Consequently, the following equality is maintained:

$$T_t^{D,in} = T_t^{C,out} = T_t^{DH,in}. \quad (13)$$

D. Control framework

The IES subsystems are operated with the objective of maximizing revenue through electricity and hydrogen generation while fulfilling local heating requirements. This paper presents a novel design configuration that connects the HTSE and DH applications in a cascade arrangement, aiming to enhance system efficiency and performance. The focus is on developing a control strategy for this configuration to ensure the DH system meets demand constraints by

regulating steam distribution in the steam manifold and controlling TES charging and discharging. The optimization problem to maximize revenue will be addressed in future research.

The heat recovered from the HTSE exhaust in HX1 may not always be sufficient to meet the heating demand. To address this, an additional line is extended from the steam manifold to directly supply topping steam to HX2. However, controlling this direct steam can impact the secondary flow distribution and introduce unwanted transients to the secondary side of the SMR. Therefore, it is desirable to limit the number of control actions and manage short-term energy balance by controlling the TES. In this paper, we assume that the topping steam can be adjusted once per day. The daily setpoint for the topping steam will provide the deficit net energy to maintain the DH supply at the target temperature. The setpoint for the topping steam flow toward DH system $\dot{m}^{DH}$ for the interval 0 to τ is given by

$$\dot{m}_{\tau}^{DH} = \begin{cases} 0 & \text{if } \int_0^{\tau} q_t^{HX1} dt \geq \int_0^{\tau} q_t^{dem} dt, \\ \dfrac{\int_0^{\tau} (q_t^{dem} - q_t^{HX1}) dt}{\tau c^p} & \text{otherwise.} \end{cases} \tag{14}$$

The charging and discharging mass flow rate of the TES is then controlled to satisfy supply-demand balance at every time step. Specifically, the thermal energy storage (TES) charges by storing excess thermal power when the heat available from the exhaust of HTSE, q_t^{HX1}, and topping steam, q_t^{HX2}, exceeds the demand, q_t^{dem}. On the contrary, TES discharges by releasing thermal power when the sum of q_t^{HX1} and q_t^{HX2} is less than q_t^{dem}. Given the thermal power utilized from the HTSE exhaust (q_t^{HX1}) and the topping steam (q_t^{HX2}), the control setpoints for TES charging and discharging mass flow rates are given by

$$\dot{m}_t^{char} = \begin{cases} 0 & \text{if } q_t^{HX1} + q_t^{HX2} \leq q_t^{dem}, \\ \dfrac{q_t^{HX1} + q_t^{HX2} - q_t^{dem}}{c^p \eta^{char} (T_t^{DH,out} - T_t^{c,out})} & \text{otherwise,} \end{cases} \tag{15}$$

$$\dot{m}_t^{dis} = \begin{cases} \dfrac{q_t^{dem} - q_t^{HX1} - q_t^{HX2}}{c^p \eta^{dis} (T_t^{D,out} - T_t^{D,in})} & \text{if } q_t^{HX1} + q_t^{HX2} \leq q_t^{dem}, \\ 0 & \text{otherwise.} \end{cases} \tag{16}$$

Equations (14)–(16) are used to calculate the setpoints for the topping steam supplied to the DH system, as well as the charging and discharging flow rates for the TES in the scenarios presented in Sec. III.

III. CASE STUDIES

In this section, the simulation of the integrated energy system with cascaded heating applications is presented. The objective is to maintain a desired DH supply temperature through the utilization of the exhaust steam from the HTSE, the topping steam directly extracted from the steam manifold, and the TES. We examine the feasibility of this design by considering a varied 24-h DH demand profile as shown in Fig. 4.

Figure 4 shows the DH demand in terms of mass flow rate of the working fluid. This demand can be converted into heat demand in kWth as

$$q_t^{dem} = \dot{m}_t^{pipe} c^p (T_{rat}^{DH,out} - T_{rat}^{DH,in}), \tag{17}$$

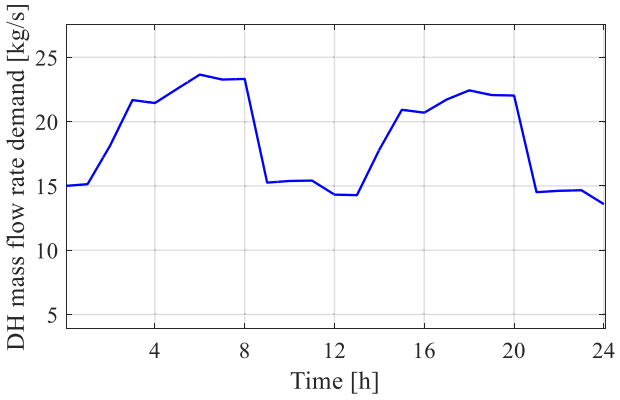

FIG. 4. The 24-h district heating demand profile in terms of mass flow rate. Data source: Poudel and Gokaraju.[12]

where $T_{rat}^{DH,out} = 90$ and $T_{rat}^{DH,in} = 40\,^{\circ}\text{C}$ are the rated supply and return water temperatures of the DH system.

A. Simulation overview

The case studies explore the operation of the IES described in Sec. II. To validate our hypothesis that the residual heat from the HTSE exhaust can be used for DH application, we have developed an IES model with cascaded heating design. In this design, the DH system is fed with heating fluids from HTSE exhaust at HX1 and topping steam from steam manifold at HX2 and has a thermal energy storage to provide balance and maintain temperature quality on a continuous basis. The IES model is developed using the Modelica programming language in the Dymola environment. Dymola is a multi-domain modeling and simulation environment that enables creation and simulation of complex physical models that integrate different domains such as mechanics, electrical, thermal, and fluid systems.[32]

The heat demand used in our analysis is drawn from Poudel and Gokaraju,[12] and we scaled it down to match the rated capacity of our IES components.

We have simulated three different scenarios to validate the hypothesis. In scenario 1, we have utilized only the exhaust steam from HTSE at HX1 for the DH system. In scenario 2, we supplement the exhaust steam from HTSE by extracting a certain amount of topping heat (topping steam) directly from the steam manifold to meet the energy requirement of the DH system. In scenario 3, we utilize the TES, in addition to the heat from the HTSE exhaust and topping steam from the steam manifold, to maintain the desired DH supply temperature. The details of the simulation results are presented in the following subsections.

B. Simulation results

The system is simulated for 24 h with the DH demand profile shown in Fig. 4. Because the objective of this paper is to demonstrate the modeling and simulation of the cascaded heating design to support the district heating demand, we have kept the SMR thermal power generation and the HTSE process at a constant rated condition throughout the simulation period in all three scenarios. This means that the steam generators produce constant 84 kg/s of steam flow at

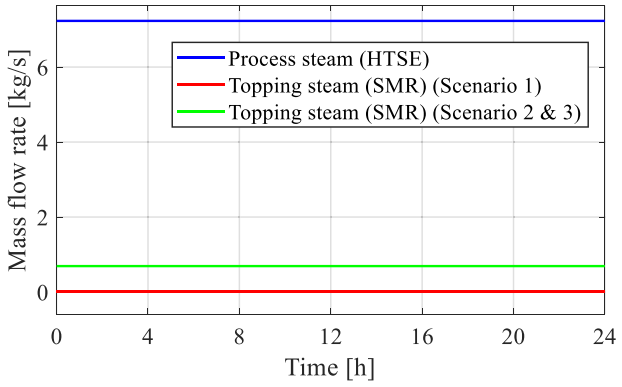

FIG. 5. Mass flow rates of the HTSE exhaust steam and the topping steams supplied to the DH system.

310 °C. The HTSE process extracts 7.23 kg/s of process steam and consumes 53.3 MWe of electricity throughout the 24-h period. A small portion of the topping steam produced by the steam generator is supplied as topping steam to the DH system (in scenarios 2 and 3), while the remaining steam is directed to the BOP to generate electricity.

Figure 5 presents the mass flow rates of the process steam to HTSE ($\dot{m}_t^{HTSE}$) and topping steam flow to the DH system ($\dot{m}_t^{DH}$) for all three scenarios. In all three scenarios, the entire flow from HTSE exhaust is supplied to the HX1 (i.e., $\dot{m}_t^{HX1} = \dot{m}_t^{HTSE}$). Figure 6 plots the actual thermal energy supplied to the DH load during the simulated 24-h period along with the actual thermal energy demand ($\dot{q}_t^{dem}$) during the same period. Figure 7 plots and compares the DH supply temperatures ($T_t^{DH,out}$) and DH return temperatures ($T_t^{DH,in}$) for the three scenarios.

1. Scenario 1: Cascaded heat recovery

In this scenario, we investigate the use of exhaust steam from HTSE for district heating in the IES. The DH system relies on the heat recovered from the HTSE process and assume that no other heat is added. The objective is to determine whether the recovered heat from the HTSE process is adequate to meet the DH load profile shown in Fig. 4.

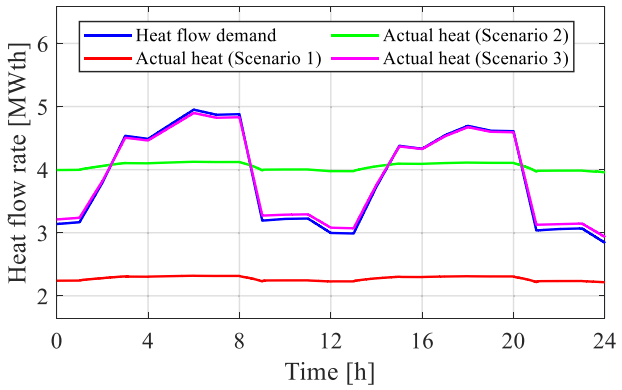

FIG. 6. Heat demand and the actual heat supplied to the DH system.

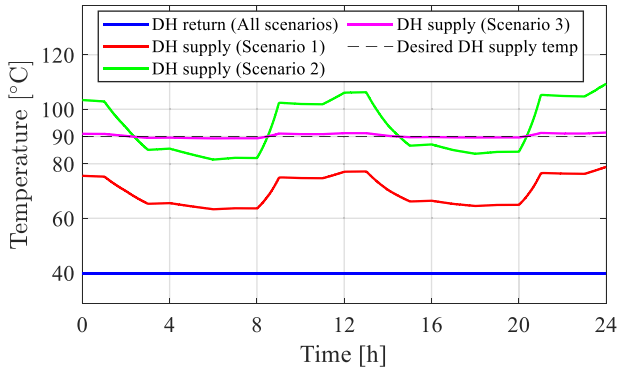

FIG. 7. Temperatures of the supply and return water of the DH system.

As shown in Fig. 5 the mass flow rate from HTSE exhaust for scenario 1 is 7.23 kg/s, which is same for other two scenarios. However, the mass flow rate of the topping steam from steam manifold for scenario 1 is zero.

When relying solely on the heat from the HTSE exhaust, the heat supplied to the DH load is always less than the heat demand, as shown in Fig. 6. As a result, the supply temperature fluctuates around 70 °C, as shown in Fig. 7. This clearly shows that the heat recovered from the HTSE exhaust alone is not sufficient to meet the DH demand, and the DH temperature continuously varies, falling below the desired temperature (i.e., 90 °C). The return temperature remains constant at preset value of 40 °C.

The results indicate the need for additional heat input to maintain the DH supply temperature at 90 °C.

2. Scenario 2: Supplementing with the process heat

The results from scenario 1 showed that the residual heat from the HTSE exhaust alone is not sufficient to meet the given heat demand. Therefore, in this scenario, the DH system extracts a small quantity of steam (topping steam) from the steam manifold at HX2.

The topping steam flow setpoint for the DH system ($\dot{m}_\tau^{DH}$) is calculated using Eq. (14) to compensate for the energy deficit. As explained in Sec. II A, this topping steam flow remains constant throughout the day to minimize control actions on the SMR side.

As depicted in Fig. 5, the mass flow rate of HTSE exhaust supplied to the DH system remains constant at 7.23 kg/s, which is the same as in scenario 1. However, the topping steam flow is increased to 0.69 kg/s. As a result, the heat supplied to the DH system in scenario 2 is greater than in scenario 1, as shown in Fig. 6. However, it still fails to meet the heat demand during peak periods and exceeds the required heat during low-demand periods.

Compared to scenario 1, the additional heat from the topping steam elevates the DH supply temperature to near 90 °C, which is our target setpoint. However, the DH supply temperature occasionally falls below the desired setpoint, particularly during peak hours, due to insufficient heat supply during those periods. The simulation results show that while the supplementary steam from the SMR can increase the DH supply water temperature to around 90 °C, the temperature

fluctuates over time around the desired setpoint due to temporal variations in the DH demand.

3. Scenario 3: Using thermal energy storage

The scenario 2 results show that relying solely on the heat from the HTSE exhaust and topping steam cannot maintain the DH supply at a desired temperature to meet the expected end-use heat quality. This scenario therefore investigates the role of TES to provide the necessary energy balance in order to regulate the DH supply temperature at a desired level. The simulation is performed using the same 24-h DH demand profile as in the previous scenarios. The mass flow from HTSE exhaust and topping steam toward the DH system are kept unchanged from scenario 2. However, the TES is activated to absorb excess heat during low demand periods and release it during high demand periods.

Figure 8 plots the charging and discharging mass flow rates of the TES during the 24-h simulation. The charging and discharging flow profiles closely follow the hourly setpoints. The charging and discharging flow setpoints shown in Fig. 8 are calculated with an hourly interval using Eqs. (15) and (16). By comparing Fig. 8 with the demand profile in Fig. 4, we observed that charging actions mainly occurs during low-demand periods, whereas discharging actions occur during high-demand periods. Figure 6 shows that the heat demand from the DH system is consistently fulfilled in this scenario with the help of TES.

Similar to the previous scenarios, the supply and return temperatures of the DH system are visualized for the 24-h simulation period as shown in Fig. 7. The plots shows that the supply temperature is consistently maintained close to 90 °C (i.e., the target temperature) throughout the 24-h period.

The simulation results show that by using TES, the DH supply can be maintained at a desired temperature. The charging and discharging of the TES are coordinated, storing excess heat during low demand periods and releasing it during high demand periods. Due to this intermittent charging and discharging processes, the temperature of different layers of TES storage materials fluctuates over time, as shown in Fig. 9. It can be seen that the temperature of the two hot layers increases, while the temperature of the two cold layers decreases by the end of the 24-h period. Additionally, the average temperature

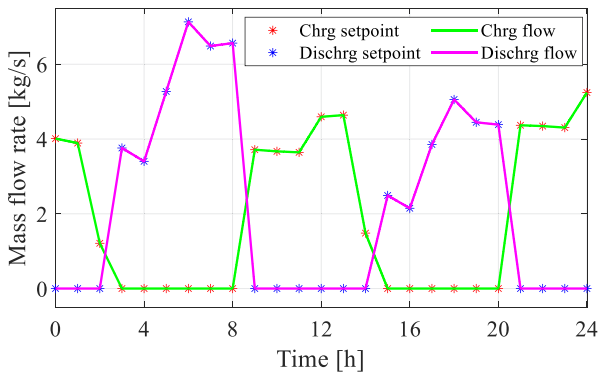

FIG. 8. Hourly setpoints and actual mass flow rate profiles of charging/discharging flows of the TES in scenario 3.

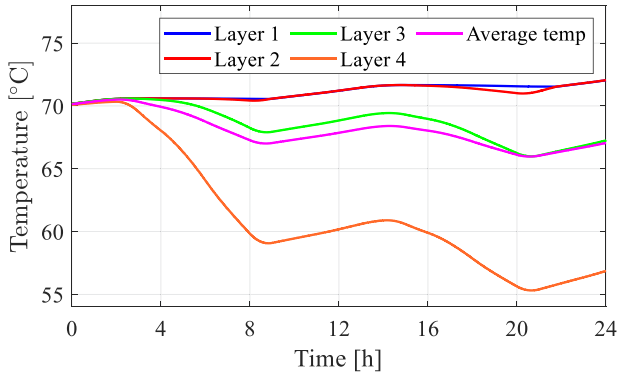

FIG. 9. Temperatures of the working fluid of different TES layers during the 24-h simulation in scenario 3. Note that we use the average temperature T_t^{TES} to calculate charging and discharging flow serpoints for simplicity [see Eqs. (11) and (12)].

T_t^{TES} at the end of the simulation is slightly lower than that at the start of the simulation. This temperature offset can be reduced by implementing more accurate setpoint controls.

In summary, by using TES in addition to the heat from HTSE exhaust and topping steam, we are able to maintain a desired DH supply temperature, thereby improving the efficiency and flexibility of the IES system.

IV. CONCLUSION AND FUTURE WORKS

This study investigated the technical feasibility of using IES to meet end-use heat demand of a district heating network by cascaded utilization of process steam from an SMR. In the proposed heating design, we used residual heat from the HTSE exhaust in combination with the topping heat from a small amount of steam extracted directly from the steam manifold to provide heat to the DH system. TES is used to maintain supply-demand balance and regulate DH supply temperature at a desired level. We developed a high-fidelity physics-based model of the IES using the Modelica language and conducted 24-h simulations to evaluate the proposed design. We investigated three different scenarios to evaluate the feasibility and effectiveness of the proposed design.

Our study concluded that the integration of an IES with cascaded heat utilization and TES presented a promising solution for efficiently meeting district heating demand and providing a stable heat supply. By combining the residual heat from HTSE exhaust and supplementary heat from the steam manifold, our proposed design enabled an effective utilization of energy resources and resulted in enhancement of the flexibility and reliability of the integrated energy system.

Specifically, our investigation involved three different scenarios to evaluate the feasibility and effectiveness of the proposed design. In scenario 1, we found that relying solely on the residual heat at the HTSE exhaust was insufficient to meet the DH demand, and the DH supply temperature fell below 90 °C. In scenario 2, the addition of supplementary heat from the topping steam successfully met the net energy requirement, but the DH supply temperature fluctuated due to varying demand. In scenario 3, the incorporation of TES proved to be instrumental in regulating the DH supply temperature and maintaining a stable and constant heat supply throughout varying demand profiles.

In the future, we will develop an optimal operation framework to optimize the steam distribution across all IES components, including DH, HTSE, and BOP, considering variable DH demand and fluctuating prices of hydrogen and electricity. By implementing this optimization framework, we will gain valuable insights into the design and operation of practical integrated energy systems and ensure efficient and cost-effective utilization of energy resources. Furthermore, we will explore steam extraction from multi-stage turbine setup to improve the efficiency of Rankine cycle and maximize overall heat utilization. This research will advance nuclear-powered IES for reliable and efficient electricity generation and heat usage. In addition, we will investigate the impacts of both short-term and long-term heat demand variations on the temperature distributions in the thermocline TES, as the effects could provide valuable insights into system efficiency and economic performance.[41,42]

ACKNOWLEDGMENTS

This work was supported through the Idaho National Laboratory (INL) Laboratory Directed Research & Development (LDRD) Program under U.S. Department of Energy (DOE) Idaho Operations Office under Contract No. DE-AC07-05ID14517.

AUTHOR DECLARATIONS

Conflict of Interest

The authors have no conflicts to disclose.

Author Contributions

Bikash Poudel: Conceptualization (equal); Data curation (equal); Formal analysis (equal); Investigation (equal); Methodology (equal); Software (equal); Validation (equal); Visualization (equal); Writing – original draft (equal); Writing – review & editing (equal). **Mukesh Gautam:** Software (equal); Validation (equal); Visualization (equal); Writing – original draft (equal); Writing – review & editing (equal). **Binghui Li:** Conceptualization (equal); Funding acquisition (equal); Investigation (equal); Resources (equal); Supervision (equal); Writing – original draft (equal); Writing – review & editing (equal). **Jianqiao Huang:** Writing – original draft (equal). **Jie Zhang:** Funding acquisition (equal); Supervision (equal); Writing – original draft (equal); Writing – review & editing (equal).

DATA AVAILABILITY

The data supporting the findings of this study are available from the corresponding author upon reasonable request.

REFERENCES

[1]Office of Federal Register. "Executive order on tackling the climate crisis at home and abroad," Federal Register 86 (2021).
[2]U.S. Energy Information Administration, see https://www.eia.gov/outlooks/aeo/ for "Annual energy outlook 2023" (2022); accessed 23 April 2023.
[3]National Academies of Sciences, Engineering, and Medicine. *Accelerating Decarbonization of the U.S. Energy System* (The National Academies Press, Washington, DC, 2021).
[4]U.S. Department of Energy, see https://www.energy.gov/eere/doe-industrial-decarbonization-roadmap for "Industrial decarbonization roadmap" (2022); accessed 23 April 2023.
[5]S. M. Bragg-Sitton, R. Boardman, C. Rabiti, and J. O'Brien, "Reimagining future energy systems: Overview of the us program to maximize energy utilization via integrated nuclear-renewable energy systems," Int. J. Energy Res. **44**, 8156–8169 (2020).
[6]G. Locatelli, A. Fiordaliso, S. Boarin, and M. E. Ricotti, "Cogeneration: An option to facilitate load following in small modular reactors," Prog. Nucl. Energy **97**, 153–161 (2017).
[7]D. Ingersoll, Z. Houghton, R. Bromm, and C. Desportes, "Nuscale small modular reactor for co-generation of electricity and water," Desalination **340**, 84–93 (2014).
[8]J. S. Kim, R. D. Boardman, and S. M. Bragg-Sitton, "Dynamic performance analysis of a high-temperature steam electrolysis plant integrated within nuclear-renewable hybrid energy systems," Appl. Energy **228**, 2090–2110 (2018).
[9]J. Rahman, R. A. Jacob, and J. Zhang, "Harnessing operational flexibility from power to hydrogen in a grid-tied integrated energy system," in *International Design Engineering Technical Conferences and Computers and Information in Engineering Conference* (American Society of Mechanical Engineers, 2022), Vol. 86229, p. V03AT03A022.
[10]T. J. Lindroos, E. Pursiheimo, V. Sahlberg, and V. Tulkki, "A techno-economic assessment of nuscale and DHR-400 reactors in a district heating and cooling grid," Energy Sources, Part B **14**, 13–24 (2019).
[11]Z. Dong and Y. Pan, "A lumped-parameter dynamical model of a nuclear heating reactor cogeneration plant," Energy **145**, 638–656 (2018).
[12]B. Poudel and R. Gokaraju, "Optimal operation of SMR-RES hybrid energy system for electricity & district heating," IEEE Trans. Energy Convers. **36**, 3146–3155 (2021).
[13]B. Poudel and R. Gokaraju, "Small modular reactor (SMR) based hybrid energy system for electricity & district heating," IEEE Trans. Energy Convers. **36**, 2794–2802 (2021).
[14]J. Rahman and J. Zhang, "Multi-timescale operations of nuclear-renewable hybrid energy systems for reserve and thermal product provision," J. Renewable Sustainable Energy **15**, 025901 (2023).
[15]R. A. Jacob, J. Rahman, and J. Zhang, "Dynamic modeling and simulation of integrated energy systems with nuclear, renewable, and district heating," in *2021 North American Power Symposium (NAPS)* (IEEE, 2021), pp. 1–6.
[16]M. F. Ruth, O. R. Zinaman, M. Antkowiak, R. D. Boardman, R. S. Cherry, and M. D. Bazilian, "Nuclear-renewable hybrid energy systems: Opportunities, interconnections, and needs," Energy Convers. Manage. **78**, 684–694 (2014).
[17]S. Werner, "International review of district heating and cooling," Energy **137**, 617–631 (2017).
[18]International Atomic Energy Agency. *Advanced Applications of Water Cooled Nuclear Power Plants* (International Atomic Energy Agency, 2008).
[19]R. A. Jacob and J. Zhang, "Modeling and control of nuclear–renewable integrated energy systems: Dynamic system model for green electricity and hydrogen production," J. Renewable Sustainable Energy **15**, 046302 (2023).
[20]G. He, D. S. Mallapragada, A. Bose, C. F. Heuberger-Austin, and E. Gençer, "Sector coupling via hydrogen to lower the cost of energy system decarbonization," Energy Environ. Sci. **14**, 4635–4646 (2021).
[21]J. D. Holladay, J. Hu, D. L. King, and Y. Wang, "An overview of hydrogen production technologies," Catal. Today **139**, 244–260 (2009).
[22]H. Lund, S. Werner, R. Wiltshire, S. Svendsen, J. E. Thorsen, F. Hvelplund, and B. V. Mathiesen, "4th generation district heating (4GDH): Integrating smart thermal grids into future sustainable energy systems," Energy **68**, 1–11 (2014).
[23]H. Gadd and S. Werner, "Achieving low return temperatures from district heating substations," Appl. Energy **136**, 59–67 (2014).
[24]X. Wang, A. Christ, K. Regenauer-Lieb, K. Hooman, and H. T. Chua, "Low grade heat driven multi-effect distillation technology," Int. J. Heat Mass Transfer **54**, 5497–5503 (2011).
[25]Y. Shatilla, "7 - nuclear desalination," in *Nuclear Reactor Technology Development and Utilization*, Woodhead Publishing Series in Energy, edited by S. U.-D. Khan and A. Nakhabov (Woodhead Publishing, 2020), pp. 247–270.
[26]A. Hauch, S. D. Ebbesen, S. H. Jensen, and M. Mogensen, "Highly efficient high temperature electrolysis," J. Mater. Chem. **18**, 2331–2340 (2008).
[27]J. O'brien, J. Hartvigsen, R. Boardman, J. Hartvigsen, D. Larsen, and S. Elangovan, "A 25 kW high temperature electrolysis facility for flexible

hydrogen production and system integration studies," Int. J. Hydrogen Energy **45**, 15796–15804 (2020).
[28]D. B. Gingerich and M. S. Mauter, "Quantity, quality, and availability of waste heat from united states thermal power generation," Environ. Sci. Technol. **49**, 8297–8306 (2015).
[29]X. Wang, M. Jin, W. Feng, G. Shu, H. Tian, and Y. Liang, "Cascade energy optimization for waste heat recovery in distributed energy systems," Appl. Energy **230**, 679–695 (2018).
[30]T. Wang, Y. Zhang, Z. Peng, and G. Shu, "A review of researches on thermal exhaust heat recovery with Rankine cycle," Renewable Sustainable Energy Rev. **15**, 2862–2871 (2011).
[31]M. Yang, S. Y. Lee, J. T. Chung, and Y. T. Kang, "High efficiency H_2O/LiBr double effect absorption cycles with multi-heat sources for tri-generation application," Appl. Energy **187**, 243–254 (2017).
[32]D. Brück, H. Elmqvist, S. E. Mattsson, and H. Olsson, "Dymola for multi-engineering modeling and simulation," in *Proceedings of Modelica* (Citeseer, 2002), Vol. 2002.
[33]Idaho National Laboratory, see https://github.com/idaholab/HYBRID/wiki for "Hybrid systems modeling and simulation" (2017).
[34]J. N. Reyes, Jr., "Nuscale plant safety in response to extreme events," Nucl. Technol. **178**, 153–163 (2012).
[35]K. Frick and S. Bragg-Sitton, "Development of the nuscale power module in the INL modelica ecosystem," Nucl. Technol. **207**, 521–542 (2021).
[36]K. L. Frick, A. Alfonsi, C. Rabiti, and D. M. Mikkelson, "Hybrid user manual," Technical Report (Idaho National Laboratory, Idaho Falls, ID, 2022).
[37]J. S. Kim, S. M. Bragg-Sitton, and R. D. Boardman, "Status report on the high-temperature steam electrolysis plant model developed in the modelica framework (FY17)," Technical Report INL/EXT-17-43056 (Idaho National Laboratory, 2017).
[38]H. Bastida, C. E. Ugalde-Loo, M. Abeysekera, M. Qadrdan, J. Wu, and N. Jenkins, "Dynamic modelling and control of thermal energy storage," Energy Procedia **158**, 2890–2895 (2019).
[39]J.-L. Scartezzini, "Computer model of an hot water stratified storage with heat exchanger," in *Passive and Low Energy Architecture*, edited by S. Yannas (Pergamon, 1983), pp. 677–684.
[40]Z. Yi, Y. Luo, T. Westover, S. Katikaneni, B. Ponkiya, S. Sah, S. Mahmud, D. Raker, A. Javaid, M. J. Heben, and R. Khanna, "Deep reinforcement learning based optimization for a tightly coupled nuclear renewable integrated energy system," Appl. Energy **328**, 120113 (2022).
[41]A. Dahash, F. Ochs, and A. Tosatto, "Techno-economic and exergy analysis of tank and pit thermal energy storage for renewables district heating systems," Renewable Energy **180**, 1358–1379 (2021).
[42]S. S. M. Tehrani, M. Saffar-Avval, S. B. Kalhori, Z. Mansoori, and M. Sharif, "Hourly energy analysis and feasibility study of employing a thermocline TES system for an integrated CHP and DH network," Energy Convers. Manage. **68**, 281–292 (2013).